

Detection of nanoparticles by means of reflection electron energy loss spectroscopy depth profiling

M. Menyhard

Institute for Technical Physics and Materials Science, Research Centre for Natural Sciences,
Hungarian Academy of Sciences, Hungary POB 17, H-1525

Published in: J. Phys. D: Appl. Phys. 46 (2013) 415304

Abstract

The various studies of nanoparticles are of great importance because of the wide application of nanotechnology. The shape and structure of the nanoparticles can be determined by transmission electron microscopy (TEM) while their chemistry by electron energy loss spectroscopy (EELS). TEM sample preparation is an expensive and difficult procedure, however. Surface sensitive, analytical techniques, like Auger electron spectroscopy (AES), X-ray photoelectron spectroscopy (XPS) are well applicable to detect the atoms that make up the nanoparticles, but cannot tell whether particle-formation occurred. On the other hand, reflection electron loss spectroscopy (REELS) probes the electronic structures of atoms, which are strongly different for the atoms being in solution or in precipitated form. If the particle size is in the nm range, plasmon resonance can be excited in it, which appears as a loss feature in REELS spectrum. Thus, by measuring AES (XPS) spectra parallel with those of REELS, besides the atomic concentrations the presence of the nanoparticles can also be identified. As an example, the appearance of nanoparticles during ion beam induced mixing of C/Si layer will be shown.

Key words: REELS, nanoparticle analysis, particle formation during Ga implantation, ion mixing

1. Introduction

The widespread application of the nanotechnology demands the wide variety of analyses of the nanoparticles appearing mostly in thin layers and/or in the surface close regions. Transmission electron microscopy (TEM) is an ideal tool for such studies; cross sectioning the sample of interest, it can image the nanoparticles. Chemical identification of the particles is also possible, because electrons travelling in a solid lose energy by inelastic interactions (plasmon loss, interband-, intraband transitions, etc.). The resultant material dependent energy losses are different enough and thus, they can be utilized for analytical purposes as well. Electron energy loss spectroscopy (EELS), applying some hundreds of keV excitation energy, is a widely used analytical tool in TEM [1]. However, sample preparation for cross sectional TEM and the measurement itself are rather difficult and expensive.

Surface sensitive analytical techniques like X-ray photoelectron spectroscopy (XPS) and Auger electron spectroscopy (AES) provide well resolved lateral and in-depth distribution of elements present in the thin layer. AES measures the electrons emitted during Auger recombination of an atom that had been ionized. The shape and energy position of the Auger peak is affected by the atomic arrangement of the excited atom, thus compound formation generally can be detected by AES. XPS measures the electrons excited by the X-ray photon. This method is extremely sensitive to the chemical binding and is applied to reveal the actual chemistry. However, the energy change accompanying particle formation (precipitation) from solution is much lower than that of the formation a chemical bond, and generally neither XPS nor AES can detect it.

Reflection electron energy loss spectroscopy (REELS), applying excitation energy up to about 10 keV, probes the electronic structure of the surface close region; its penetration is in the range of some nms. It is a widely used technique e.g. for determining the dielectric constant of the surface layer [2], measurement of the valence-electron density [3], the topography of the surface [4], ion bombardment induced damage [5], the band alignment of ultra thin gate oxide [6] etc.

In the energy range of REELS, plasmon resonance is the most intense loss process. Plasmons can only be excited (applying photons and electrons as well, but we will restrict ourselves to the electron excitation) if loosely bound conduction band electrons are present. There is some controversy concerning the minimum size of nanoparticles in which plasmons can be excited. The available minimum particle size also depends on the type of excitation; it seems that using electron excitation the minimum size for plasmon excitation is in the range of 1-2 nm of diameter. Really, Scholl et al. [7] have shown that, using good quality EELS, it is possible to detect plasmon losses in silver particles as small as those having a diameter of 1.7 nm.

REELS excites exactly the same losses as EELS (with higher cross section because of the lower excitation energy) thus it can also detect particles of diameter of 1-2 nm in the surface close region. Thus, in concert with depth profiling, REELS can be used to determine the in-depth distribution of nanoparticles.

Practically all Auger electron spectrometers use electron excitation up to 10 keV. These devices are also ideally applicable for REEL analysis; the REELS spectra can be recorded in the same equipment at the same time.

In this paper we report on parallel AES and REELS depth profiling of a C/Si layer intermixed by irradiation of 30 keV Ga^+ ions. While in a usual REELS application, the shape, position etc. of a REELS peak is measured to describe certain characteristics of the material, here we focus on the

appearance of the given REELS peak to recognize the presence of particles large enough for plasmon excitation. It will be shown that depending on the irradiation fluence, particles might appear in the affected layer. The appearance of particles cannot, however, be simply correlated to the atomic concentration and thus, the use of the REELS is inevitable.

2. Experimental

C (20 nm)/Si(20 nm)/C(20 nm)/Si(20 nm)/C(20 nm)/Si substrate multilayered specimens have been prepared by sequential sputter deposition of pure carbon and silicon on silicon (111) substrate. Both types of the layers were amorphous [8]. A 200x200 μm^2 area of the specimens were irradiated by Ga^+ of 30 keV in a LEO 1540XB (FEG SEM – FIB) cross beam system at room temperature, using the Canion FIB optics. The applied fluences, 10, 40, 60, 80, 120 $\times 10^{15}$ Ga^+/cm^2 , were determined by the time of the single pass irradiation.

STAIB DESA 105 pre-retarded cylindrical mirror analyzer (CMA) working in electron counting mode was applied to collect the spectra for AES and REELS as well. Since the analyzer's cut-of-energy is about 2500 eV for REELS the primary electron beam energy was chosen to be about 2000 eV. This energy is sufficient to excite the C(KLL), Si(LVV), Ga (MNN) Auger peaks thus, we could measure all relevant Auger lines together with the loss peaks.

Our standard depth profiling technique, that is, sequential AES and REELS analysis and ion removal steps were applied. For ion removal Ar^+ ions were used with energy of 1 keV, and 80° angle (with respect the surface normal) of incidence. During ion bombardment the sample was rotated (2 rpm). Using such ion bombardment conditions the disadvantageous bombardment induced roughening and ion mixing are minimized [9], and depth resolution in the range of some nms can be achieved.

2.1 Evaluation of AES and REELS spectra

The simple relative sensitivity factor method was applied for the evaluation of the AES as is described in ref [8].

For the evaluation of the REELS spectra a rough approximation was used; it was supposed that the measured loss function is a weighted (by the concentration) sum of the loss functions of the components. For this procedure, the loss spectra of the assumed components, those of Si, SiC, Ga, C had to be determined.

Ga irradiation only affects the first C and following Si layers and thus, the second C and following Si layer are pure amorphous Si and C regions; the corresponding loss spectra were taken from those regions. In the surroundings of the deeper laying C/Si interfaces, which were not affected by the Ga irradiation SiC could be detected. The SiC loss spectrum could be determined in this region. (This compound formation might have occurred during the growth of the layer system and/or was induced by the ion bombardment used in depth profiling.) The SiC REELS spectrum was also measured on single crystal SiC; this spectrum differed slightly from that measured on the C/Si interface. This is not a surprise since it has been shown earlier that the loss features of SiC change due to various defect structures [5]. Applying large enough fluence ($80 \times 10^{15} \text{ Ga}^+ \text{ ions/cm}^2$) at a depth of about 19 nm only two species those of SiC and Ga can be found. Knowing the loss spectrum of SiC the loss spectrum of Ga could thus be derived. The loss spectra (fitted to have roughly the same height) determined in this way are shown in figure 1.

The plasmon energy, E_p , can be calculated in the free-electron approximation as $E_p = \hbar(4\pi\rho e^2/M)^{1/2}$, where, ρ is the electron density and M is the electron mass to be 16.5 eV, 25.5 eV, 21 eV and 13.5 eV for Si, C (amorphous), SiC and Ga, respectively. These values are also shown in figure 1.

Having these functions, a simple linear procedure was applied to find the intensities of the components for fitting the measured loss function. During this procedure, called decomposition, the energy position of the Si, Ga, and C loss spectra were fixed. The energy position of the SiC loss peak was allowed to change within a range of 1 eV, since it is known that due to various defects [5] the energy of the SiC loss peak changes, and during depth profiling and Ga⁺ irradiation various depth dependent defect productions take place.

The cross section of plasmon excitation is material dependent, thus the intensities determined by the decomposition do not provide directly the concentrations of the components. To find the concentrations, we applied the same relative sensitivity factor method, which is used in the case of AES spectra. Thus, the concentration, c_i , of component i is $c_i = (I_i / \alpha_i) / \sum I_i / \alpha_i$ where I_i and α_i are the measured intensity and relative sensitivity factor of component i , respectively. The determination of sensitivity factors for Si, SiC and C is straightforward since the loss functions could be measured on pure materials. For Ga the sensitivity factor was chosen supposing that all Ga at a given depth is in particle form. This assumption might cause a systematic error, which on the other hand does not affect the comparison of the results.

3. Results

Figure 2 shows the conventional AES depth profile, that is, the atomic concentrations as a function of depth, recorded on a sample which was intermixed by applying an ion irradiation of 80×10^{15} Ga⁺ ions/cm², having energy of 30 keV. Figure 3 shows the REELS depth profile recorded parallel with the AES depth profile; it shows the concentrations of the energy loss components as a function of depth. The sample, parameters of ion bombardment and depth scales of figure. 2 and figure. 3 are, evidently, identical.

4. Discussion

The effective attenuation lengths (EAL) of the signal electrons give the average thickness of the analyzed area (information depths). The EAL-s for Ga 56 eV, Si 92 eV and C 272 eV Auger electrons in matrixes of C and Si were calculated applying the program given by ref [10], and inelastic mean free paths (IMFP) from ref [11] to be about 0.5, 0.5 and 1 nm, respectively. In the case of REELS, the mean penetration depth characterize the same quantity which was found to be about 1.5 nm for the applied 2000 eV primary beam energy, using the IMFP values of ref [11].

Ion bombardment applied for depth profiling causes ion mixing and surface roughening resulting in the broadening of the interfaces; the resulting depth resolution is around 1-2 nm [9]. Thus, based on the above, we can estimate that the depth resolution of the analyzing methods, either AES or REELS depth profiling, is in the range of 2-3 nm. According to figure 2 and 3 concentrations are slowly varying functions of the depth. It follows that all corrections, due to the finite depth resolution of the analyzing methods, can be neglected and we can state that the two methods, AES and REELS, probe the same volume.

The AES depth profile, figure 2, clearly shows that the first C and following Si layers had been completely intermixed by the Ga⁺ irradiation. A large amount of Si was transported to the originally pure C layer and similarly considerable amount of C was transported to the originally pure Si layer. Part of the intermixed C and Si atoms reacted (nominally at room temperature) forming SiC, which could be detected by measuring the changes of the shapes and energy positions of the C (KLL, ~ 272 eV) and Si (LVV, ~92 eV) Auger peaks. It is also clear that besides the original elements, a large amount of implanted Ga also appeared in the intermixed

layer. It can be also concluded by varying the fluence of irradiation that the amount of the SiC produced scales with the square root of fluence, etc; all these results are discussed in detail in [8]. Figure 3 shows the REELS depth profile. It is evident that the atomic distribution depth profile imaged by AES and the in-depth distribution of the particles imaged by REELS are strongly different.

To check the differences in detail, the corresponding REELS and AES depth profiles will be compared, in figures 4- 7.

According to the AES depth profile (figure 4), there is a large amount of implanted Ga in the intermixed layer forming a wide Ga distribution, spanning from the surface until a depth of about 36 nm. The distribution measured by the AES is close to that which is predicted by the Dynamic Transport of Ion in Solid (TRIDYN) code [8, 12], that is, the measured Ga profile is realistic one. The in-depth distribution of the Ga loss peak revealed by REELS measurement, that is, the distribution of the Ga particles (large enough to facilitate plasmon excitation) is significantly different from the elemental distribution, and it is much thinner. No Ga particles were observed up to a depth of about 15 nm, where the Ga concentration is as high as 45 at %. From this depth, the concentration of Ga particles increases and can be observed until a depth of 35 nm. At this depth the Ga concentration is only 10 at %, however. Thus, we conclude that there is no clear correlation between the concentration of Ga atoms and particle formation. This can be accepted if one considers that during Ga irradiation there is a steady state condition of the particle formation depending on the rates of formation and disintegration (due to energetic Ga⁺ ions) of nanoparticles. These rates are depth dependent and might cause the missing correlation between the particle formation and atomic concentration.

Either the AES or the REELS easily separate the Si atoms being in compound or free, that is, SiC and the “non-bounded, metallic” form, respectively. Thus, we will deal separately with the two species.

Similarly to the case of Ga, there is considerable difference between the REELS and AES in-depth profiles of “metallic” Si, shown in figure 5. The original structure of the sample (before ion mixing) was as follows: 20 nm C layer on the top and 20 nm Si below it, that is, the first (counted from the surface) C/Si interface originally was at depth of 20 nm. After the Ga⁺ irradiation, Si either in SiC or in “metallic” forms, can be seen in the whole 40 nm thick region demonstrating the efficiency of the intermixing. Metallic Si can only be found in the depth region of 15-36 nm, however. The in-depth distribution of Si particles, made visible by the REELS, spans from only from 25 nm until 36nm. It follows that in the 15-25 nm depth region (where Si could be detected by AES and not by REELS) all Si is in solution. Thus, the Si atoms transported by ion mixing to the C layer did not form small precipitates, rather form carbide or remain in solution. Similarly not even the originally pure Si region (~20-25nm thick region) contains large enough particles for plasmon generation. In this region there is strong SiC formation and the remaining Si seems to be in solution. In depth region of 25-36 nm there are large enough particles for plasmon excitation, that is, part of the originally pure Si region was not completely destroyed by the ion bombardment.

Just contrary to the above, there is good correlation between AES and REELS in-depth profiles of C and SiC, shown in figure 6 and figure 7, respectively. This means that all C transported to the Si/SiC mixture forms carbide, and the carbide nucleus grow to large enough size in which plasmon excitation is possible. The loss energy of SiC varied (in a range of 1 eV) along the depth. It has been shown previously [5] that the plasmon energy of SiC depended on the ion

bombardment applied. There are several works, which prove that the loss energy might depend on the size of the particle as well [7,13,14]. At this point it is not possible to identify whether the size and/or defects structure of the SiC particles is responsible for the observed shift of the plasmon peak, but either one of them or both change along the depth.

All the above mean that the nanoparticle formation is a complicated process and generally cannot simply be estimated from the concentration of the given element, and thus performing REELS measurements is inevitable. This point will be demonstrated by the following.

The formation of Ga particles as a function of Ga^+ irradiation fluence was studied by REELS and AES depth profiling of the sample above (C (20 nm)/Si(20 nm)/C(20 nm)/Si(20 nm)/C(20 nm)/Si substrate) subjected to Ga^+ (30keV) irradiations of fluences of 10, 20, 40, 60, 80, 120 x 10^{15} ions/cm². The results are shown in figure 8, which shows the Ga atom and particle distributions belonging to various irradiations revealed by AES and REELS depth profiling.

The irradiation causes material removal as well, thus, the depth profiles (recorded from layers of various thicknesses) are shifted to fit the position of the Si/C interface (not affected by ion mixing) at a depth of 40 nm. REELS did not show any Ga loss signal if the sample was irradiated by fluences of 10, 20, 40, 60 x 10^{15} Ga^+ ions/cm². During these irradiations large amount of Ga atoms were implanted to the layer (see the concentration profiles shown by figure 8) that did not precipitate to form particles. The applied extensive irradiations caused serious intermixing which was discussed in detail in ref [8]. If the fluence was increased only by about 30% to 80 x 10^{15} ions/cm², the AES did not show any dramatic changes; the measured concentration increased slightly as it is expected. On the other hand in the REEL spectra high intensity (varying along the depth) Ga loss peak appeared. Obviously, the particle and atomic in-depth distributions are strongly different. The Ga loss peak (nanoparticles are present) appears and disappears in depths

where the atomic concentration of Ga are about 50% and 15 %, respectively. At the case of $60 \times 10^{15} \text{ Ga}^+ \text{ ions/cm}^2$ irradiation the Ga atomic concentration is larger than 35% in the depth range of 22-27 nm and decreases below 15% at a depth of 35 nm. Still in this case no Ga loss peak, particle formation was observed. At irradiation fluence of 120 ions/cm^2 the Ga atomic concentration increases as expected (with respect the irradiation of $80 \times 10^{15} \text{ ions/cm}^2$), while the concentration of particles increased more than 1.5 (the increase the fluence). Here the particles appear on the very surface where the atomic concentration is 32 % and disappear at a depth of 35 nm, where the concentration is 25%. All these data are different from those found in the case of $80 \times 10^{15} \text{ ions/cm}^2$ irradiation. These results also demonstrate that the particle formation cannot be determined by simply measuring the concentration of the implanted Ga.

REEL measurement can be carried out in any AES device and can widely be applied since plasmons can be excited in nearly all elements. These measurements provide a simple way to detect nanoparticles in thin layers with depth resolution of some nms.

4. Conclusions

It has been shown that REELS depth profiling provides information about the presence and distribution of the nanoparticles (here produced by ion mixing) large enough for facilitating plasmon excitation. The lateral and depth resolution of the method depends on the diameter of the exciting electron beam and the combined effect of the IMFP and sputter removal being in the range of nms.

As an application, a C/Si layer was intermixed by Ga^+ irradiation. Applying parallel AES and REELS depth profiling we have shown that at sufficient irradiation fluences a./ Ga nanoparticles were detected, their quantity and distribution could not be correlated with the Ga (implanted)

atom distribution, and b./ just contrary the particle distributions of the SiC and C correlate with the atomic distributions. Thus, the atomic distribution in itself is an insufficient measure of particle formation.

References

- [1] Egerton R F 2011 *Electron Energy-Loss Spectroscopy in the Electron Microscope*, Third edition, Springer
- [2] Yubero F, Sanz J M, Ramskov B and Tougaard S 1996 Phys. Rev. **B53** 9719
- [3] Strawbridge B, Singh R K, Beach C , Mahajan S and Newman N 2006 J. Vac. Sci. Tech. **A24** 1117
- [4] Katayama Y, Shimada T and Usami K 1981 Phys. Rev. Lett. **46**, 1146
- [5] Kotis L, Sulyok A, Menyhard M, Malherbe J B and Odendaal R Q 2005 Appl. Sur. Sci. **252** 1785
- [6] Shin H C, Tahir D, Seo S, Denny Y R, Oh S K, Kang H J, Heo S, Chung J G, Lee J C and Tougaard S 2012 Surf. Interface Anal. **44** 623
- [7] Scholl J A, Koh A L and Dionne J A 2012 Nature **483** 421
- [8] Barna A, Gurban S, Kotis L, Labar J, Sulyok A, Toth A L, Menyhard M, Kovac J and Panjan P 2012 Appl. Surf. Sci. **263** 367
- [9] Barna A, and Menyhard M 1994 Phys. Stat Sol. (a) **145** 263
- [10] *NIST Standard Reference Database 82 Ver.1* 2001 (Powell C J and A Jablonski), NIST Gaithersburg
- [11] Tanuma S, Powell C J and Penn D R 1994 Surf. Interf. Anal. **21** 165
- [12] TRIDYN_FZR, FZR-317, Möller W. and Posselt M., Forschungszentrum Rossendorf, 01314 Dresden, Germany.

- [13] Sato Y, Terauchi M, Mukai M, Kaneyama T and Adachi K 2011 Ultramicroscopy **111**
1381
- [14] García de Abajo F J 2010 Rev. Mod. Phys. **82** 209

Figure captions

1. The elemental REELS spectra used in the decomposition process. The vertical lines show the nominal plasmon energies for pure Ga (13.5 eV), Si (16.5eV), SiC (21 eV) and C(25.5 eV) graphite), respectively.
2. The beginning part of AES depth profile of C/Si/C/Si/C sample irradiated by $80 \times 10^{15} \text{ Ga}^+$ (30 keV) ion/cm².
3. The REELS depth profiles of the components measured parallel with the AES depth profile shown in Fig. 2; evidently the sample, irradiation, horizontal axis are identical.
4. The comparison of the REELS and AES depth profiles of Ga.
5. The comparison of the REELS and AES depth profiles of Si.
6. The comparison of the REELS and AES depth profiles of C.
7. The comparison of the REELS and AES depth profiles of SiC.
8. The Ga atom and particle distributions measured by AES and REELS, respectively for various Ga^+ (30 keV) irradiations. The fluence is given in the legend in units of $10^{15} \text{ ions/cm}^2$.

Figures

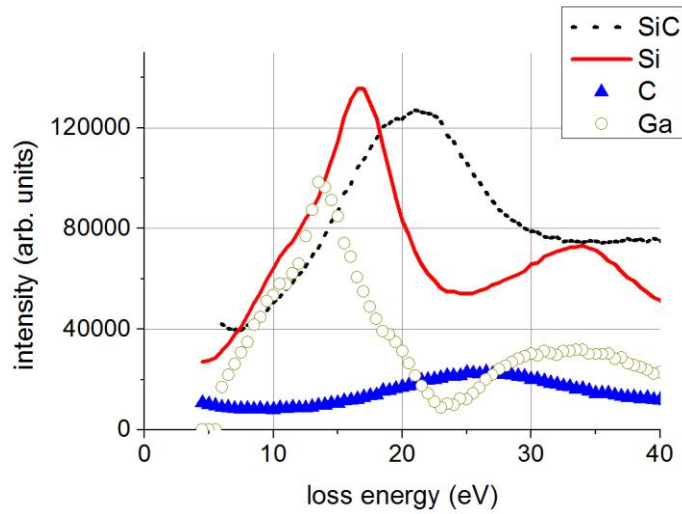


Figure 1

The elemental REELS spectra used in the decomposition process.

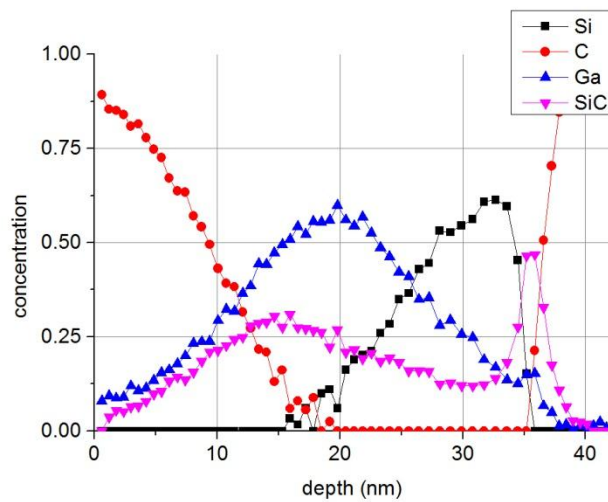


Figure 2

The beginning part of AES depth profile of C/Si/C/Si/C sample irradiated by $80 \times 10^{15} \text{ Ga}^+$ (30 keV) ion/cm^2 .

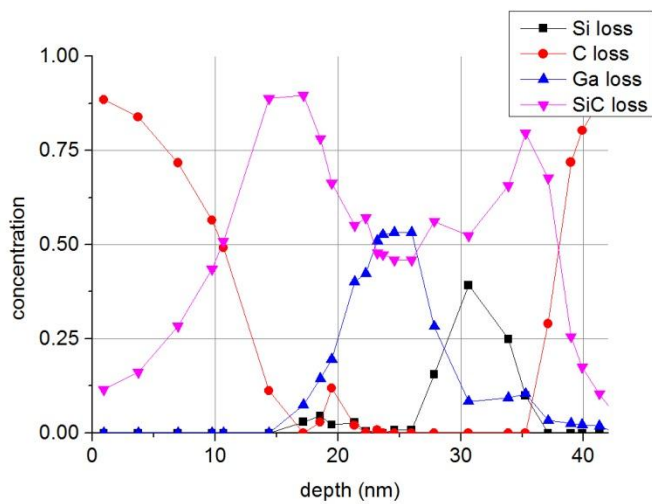


Figure 3.

The REELS depth profiles of the components measured parallel with the AES depth profile shown in Fig. 2; evidently the sample, irradiation, horizontal axis are identical.

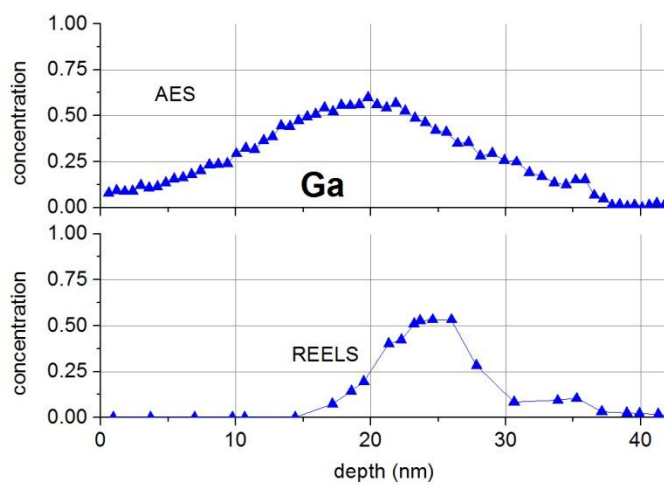


Figure 4

The comparison of the REELS and AES depth profiles of Ga.

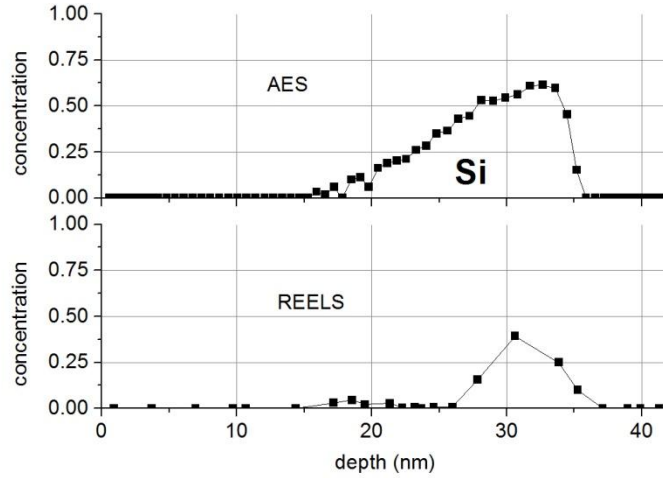


Figure 5

The comparison of the REELS and AES depth profiles of Si.

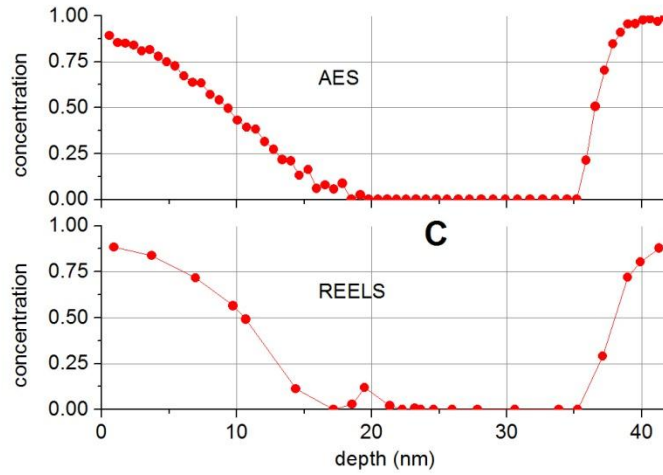


Figure 6

The comparison of the REELS and AES depth profiles of C.

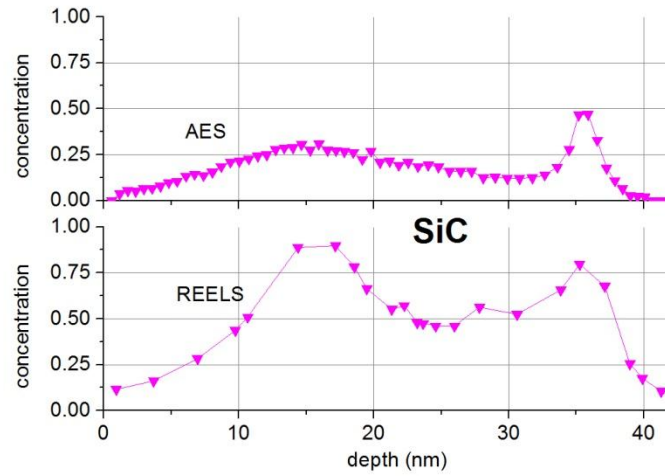


Figure 7

The comparison of the REELS and AES depth profiles of SiC.

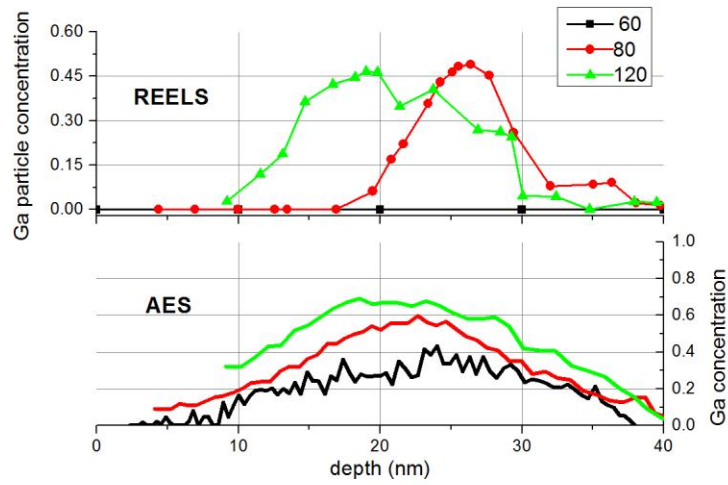


Figure 8.

The Ga atom and particle distributions measured by AES and REELS, respectively for various Ga^+ (30 keV) irradiations. The fluence is given in the legend in units of 10^{15} ions/cm².